ADVANCED ENGINEERING MATERIALS
www.aem-journal.com

Janus Paper-Based Wound Dressings for Effective Exudate Absorption and Antibiotic Delivery

*Yang Gao, Anwar Elhadad, and Seokheun Choi**

Traditional hydrophilic wound dressings, while common, fail to effectively drain wound exudate, creating conditions favorable for bacterial growth. Similarly, newer Janus-type dressings with hydrophobic-hydrophilic properties also fall short, as their hydrophobic side causes excessive dryness by pulling biofluids from the wound, disrupting moisture balance. Additionally, embedding antibiotics in dressings at fixed concentrations, regardless of the infection type, reduces effectiveness and contributes to the growing problem of antibiotic resistance. In response, a single-layered Janus paper wound dressing, designed for efficient exudate absorption and precise antibiotic delivery, is developed. The approach differs from traditional Janus-type dressings; a hydrophilic layer is placed directly against the wound for better moisture management, while antibiotics are applied through the hydrophobic layer. To further enhance exudate management, the hydrophilic section with four extra absorbent pads is extended. The dressing's antibiotic efficacy and dosage are tailored based on antibiotic susceptibility testing, ensuring targeted treatment. The selected antibiotic is manually added but automatically delivered directly to the wound bed. The in vitro and ex vivo evaluations, using bacterial cultures on agar and porcine skin assays, respectively, confirm the dressing's superior exudate drainage and its ability to inhibit pathogen growth and reproduction, marking a significant advancement in wound care.

1. Introduction

In our everyday life, skin wounds are inevitable issues frequently originating from burns, chemical and mechanical injuries, surgeries, and diabetic complications.[1,2] Most wounds heal themselves through four stages: hemostasis, inflammation, proliferation, and remodeling.[3] However, that successive and overlapping wound process can be readily hindered by microbial infections, causing chronic wounds.[4,5] In particular, the inflammatory phase is essential to successful wound healing by secreting a small amount of exudate to activate the innate immune system, which will remove potential pathogens from the wound bed.[6,7] However, excessive wound exudate during inflammation can create an ideal microenvironment for bacterial breeding and potential infections because the exudate is nutrient-rich containing many vitamins, growth factors, and leukocytes.[8,9] Traditional hydrophilic wound dressings (e.g., gauzes, bandages, and hydrogels) integrated with antibiotic substances partially improved wound healing by absorbing excessive exudate and inhibiting bacterial growth.[1,6,7,9,10] Even the emerging Janus membranes with a hydrophobic–hydrophilic interface (e.g., fiber-, sponge-, hydrogel-, and polymer-based dressings with asymmetric wettability) accelerated drainage of excessive biofluid around wounds through unidirectional water-transfer capability from the skin-facing hydrophobic side to the exposed hydrophilic side while preventing favorable conditions for bacterial growth.[11–16] Moreover, the integration of antimicrobial materials into the Janus membranes[16–20] or advanced Janus multilayer membranes for effective antibiotic delivery substantially prevented the growth and reproduction of pathogens.[21,22] However, the most critical issue that traditional and emerging wound dressings overlook is the lack of effective delivery of antibiotics that are clinically relevant. Available wound dressings are equipped with a fixed amount of selected antibiotics, which can instigate the misuse or overuse of empirically prescribed broad-spectrum antibiotics and accelerate the antibiotic resistance crisis.[23,24] Antibiotic resistance can cause significant delays in wound healing, increasing treatment costs, hospitalization, amputation risk, and even mortality.[25] Furthermore, those antibiotics in wound dressings are not specifically applied to the wound bed, creating cytotoxicity and side effects while the penetration and delivery of antibiotics through the thick dressings are not efficient decreasing the therapeutic effect.[26] Also, conventional techniques suffer from the conflicting direction of the flows between the exudate absorption and the antibiotic delivery. While the exudate is absorbed from the wound bed to the dressing, the antibiotic embedded in the dressing needs to be delivered in the opposite direction.[22] The strong capillary force of the hydrophilic dressings and the

Y. Gao, A. Elhadad, S. Choi
Bioelectronics & Microsystems Laboratory
Department of Electrical & Computer Engineering
State University of New York at Binghamton
Binghamton, NY 13902, USA
E-mail: sechoi@binghamton.edu

S. Choi
Center for Research in Advanced Sensing Technologies & Environmental Sustainability
State University of New York at Binghamton
Binghamton, NY 13902, USA

The ORCID identification number(s) for the author(s) of this article can be found under https://doi.org/10.1002/adem.202301422.

DOI: 10.1002/adem.202301422

unidirectional self-pumping of the Janus dressings significantly interfere with antibiotic delivery. Several additional critical problems come with the emerging Janus dressing techniques. Because the hydrophobic side contacts the skin and continuously pumps away the exudate, a dry microenvironment can be created near the wound bed. Usually, a balanced moisture condition is critical for wound healing by increasing the rate of reepithelialization.[7,27] Moreover, the hydrophilic side filled by exudates unidirectionally transported from the skin through the hydrophobic area is exposed to the air and vulnerable to infection by environmental bacteria. Additionally, the continuous self-pumping can be easily interrupted by the limited hydrophilic area and slow evaporation. Because the macromolecules of the exudate are thick and sticky, the hydrophobic layer frequently clogs, which reduces the initial pressure for directional exudate transport.

To address those limitations and minimize antibiotic resistance, we designed a fundamentally different Janus-type dressing on disposable, scalable, and easily wax-patternable chromatography paper (**Figure 1**a,b). While the hydrophobic side of the conventional Janus dressings faces the human skin to self-pump the wound exudate,[11–16] our Janus dressing is reversed so its hydrophilic side is placed on the skin (Figure 1a). A one-layer hydrophilic pad cannot absorb all of the exudates, so we added four more pads (i.e., hydrophilic chambers) so that a sufficient amount of wound fluids can be properly managed. Figure 1b,c shows that the production of the small dressings is scalable. The hydrophilic patterns and absorbent pads can be precisely designed to properly treat different wound types, sizes, phases, and exudate production rates. The hydrophilic pattern builds chambers and channels, and that branched network continuously absorbs and transports the exudate throughout the four pads while keeping the middle region half-wet maintaining to maintain a moist environment. The paper-based Janus wound dressing is flexible and wearable, providing conformal contact with the skin through 3M Tegaderm medical tape (Figure 1d,e). Because the wax-patterned hydrophobic side of the Janus dressing faces upward, the penetration of bacteria from the environment can be prevented. Then, through the "X" printed on the hydrophobic side, the exact dose of the right antibiotic can be introduced, which is unidirectionally and effectively delivered right to the wound bed. Therefore, the conflicting fluidic issue between the exudate absorption and drug delivery can be significantly mitigated. Evidence-based treatment guidance with appropriate antibiotics and their doses can be provided by conventional phenotypic antibiotic susceptibility testing of bacterial samples potentially extracted from the wound. That will reduce antibiotic resistance and improve antibiotic stewardship for wound healing. Innovatively, the paper material exhibits superior compatibility with wound dressing applications, as it is more affordable, readily available, biocompatible, and flexible. The easy

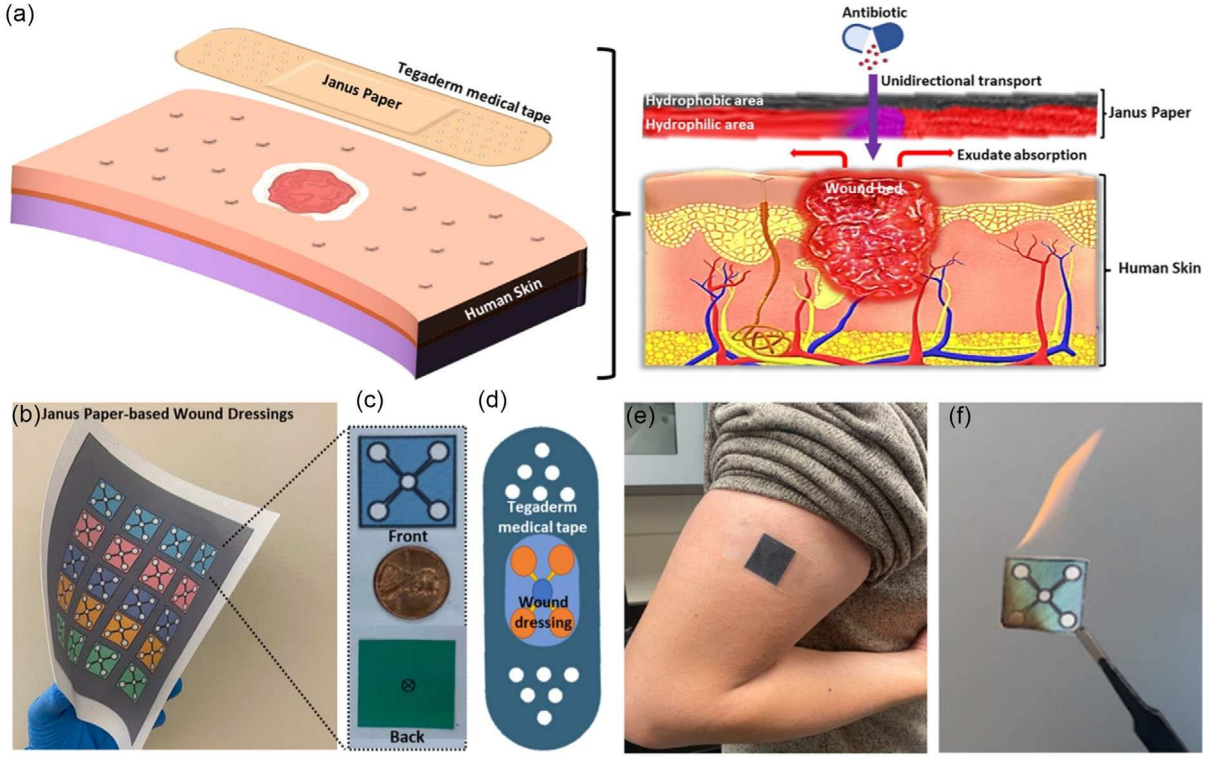

Figure 1. Comprehensive overview of the Janus wound dressing design and applications. a) Conceptual illustration showcasing the Janus wound dressing, designed for efficient exudate adsorption and unidirectional antibiotic delivery. b) Photograph displaying the Janus paper wound dressings, highlighting their scalability and potential for mass production. c) Photograph illustrating the distinct front (skin-facing) and back (air-facing) sides of the individual wound dressing unit. d) Schematic representation detailing the integration of the wound dressing with 3M Tegaderm medical tape. e) Photographic evidence of the wearable nature of the Janus paper-based wound dressing, demonstrating its practical application. f) Illustration of the environmentally safe disposal method for the device, specifically its incineration process.

disposability of paper through incineration will attract much attention as the future of wound dressings, reducing the potential risks of bacterial infection and antibiotic leakage (Figure 1f).

2. Results and Discussion

2.1. Fabrication and Characterization of Janus Paper-Based Membranes

Typically, multiple replacements of the wound dressing are required while healing.[10,13] Moreover, different functional dressings are suggested depending on the healing stages.[5,10] In that sense, paper can be a promising dressing material because of its cost-effectiveness, flexibility, disposability, biocompatibility, breathability, and easy functional integration with other materials. In particular, the simple procedure for patterning paper by wax printing and sequential heat treatment offers the transformative potential of generating various functions for paper-based devices.[28,29] Very recently, our group demonstrated the directional manipulation and retention of human sweat by controlling the wax penetration through paper, which improved the sweat collection and sensing accuracy of sweat biomarkers.[30] Here, that technique was leveraged as an innovative wound dressing for efficient exudate absorption and effective drug delivery. First, a Janus-type membrane having asymmetric wettability was created by controllably impregnating the hydrophilic paper with the hydrophobic wax. A proper heat treatment condition (150 °C for 40 s) maximized unidirectional water transport by forming an optimal hydrophobic–hydrophilic interface within a single sheet of chromatography paper.[30] To characterize the asymmetric water transport through the engineered paper and evaluate its practicability as a wound dressing, we placed a 3°μL water droplet on each of the hydrophobic and hydrophilic sides (**Figure 2**a). One of the variables that affects how liquid is transported is how the liquid is placed on the dressing. The contact angle of the droplet on the hydrophobic side was 104°, and it was transported to the hydrophilic side. In our study, the functional performance of the paper is predominantly governed by two key forces: downward hydrostatic pressure (F_H) and Laplace pressure (F_L). The hydrostatic pressure is calculated using the formula $P = \rho gh$, where P represents the pressure, ρ is the liquid density, g denotes the acceleration due to gravity, and h is the height of the liquid column. Conversely, the Laplace pressure is determined using $P = 2\gamma/r$, with γ symbolizing the surface tension and r the radius of curvature. During our controlled experiments, conducted at a consistent room temperature of 25 ± 3 °C, we considered the following parameters for water: a density (ρ) of 1.0 g cm^{-3} and a surface tension (γ) of 71°mN m^{-1}. The acceleration due to gravity (g) was taken as a constant at 9.81 m s^{-2}. Given that our experiment involved only one type of liquid, we were able to streamline the calculations as follows: We measured the height of the liquid column in contact with the dressing (h) at 0.15 cm and used the curvature of the droplet, derived from contact angle measurements, with a radius (r) of 0.12 cm. Consequently, this yielded a F_H of approximately 14.715 Pa and a F_L of approximately 118.333 Pa. F_H and F_L were sufficient to overcome the upward hydrophobic pressure (F_P) allowing the water to pass through the hydrophobic layer.[21,30,31] The downward force on the droplet became larger when the droplet entered the hydrophilic region because of the added capillary force (F_C) and the increased surface tension (F_A) with an increase in droplet size. Therefore, the thickness ratio between the hydrophobic and hydrophilic regions and the porosity change in the hydrophobic region can be the most important factor in determining the unidirectional liquid transport. In our previous report, we thoroughly evaluated the effect of the thermal treatment on those factors and maximized the capability of directional water transport.[30] On the contrary, when the droplet was placed on the hydrophilic side, its contact angle was 21° and then it spread instantly over the hydrophilic layer. The four pressures of F_H, F_L, F_A, and F_C generated a very strong downward force on the droplet, but dissipated horizontally along the hydrophilic region, letting the droplet wet the hydrophilic region only. This force was not enough to overcome F_P in the vertical upward direction so the droplet could not penetrate the hydrophobic layer below.

The droplet placed on the hydrophobic side moved through and wicked the hydrophilic side (Figure 2b–(1)). Under mechanical bending (which will happen in real life), this liquid transport capability was maintained (Figure 2b–(2)). Even when we flipped the Janus membrane and introduced the water to the hydrophobic region facing down, the water could penetrate the region against gravity and wet the hydrophilic side (Figure 2b–(3)). However, the droplet just stayed and spread along the hydrophilic region when we applied the droplet to the hydrophilic side (Figure 2b–(4)). That asymmetric wetting propriety that depends on the application direction of the liquid is critical to providing a foundation for the development of our proposed wound dressing.

2.2. Design of Janus Paper-Based Wound Dressings

To effectively absorb the wound exudate and not interfere with the drug delivery in the direction opposite to the exudate absorption, the hydrophilic region was extended to four absorbent pads with channels. Those hydrophilic chambers and channels were well-defined by wax-printing and heat treatment. We assume that the size of the wound bed is 0.264 cm^2 and the exudate release rate is 1 μL h^{-1}. The volume of the middle and each side chamber is 12.6 and 19.6 μL, respectively, reaching 91 μL in total (excluding the channels) so that the dressing can absorb the wound exudate for more than 90 h. Our conceptual wound dressing will be directly applied to the wound bed on which the dressing's side with hydrophilic patterns is placed (**Figure** 1 and **3**a). The four absorbent pads and the gradual widening of the channels can facilitate the absorption of the wound biofluid and transport it from the middle to the sides of the pads. This effective wicking and transporting capability keeps the middle hydrophilic chamber half-wet so that the antibiotic applied from the hydrophobic side of the Janus dressing can build up enough force to be unidirectionally transported and delivered to the wound bed. Based on our simulation with red (100 μL) and blue (20 μL) ink representing exudate and antibiotic, respectively, our Janus wound dressing effectively delivered the drug directly to the wound bed (Figure 3a). On the contrary, when the hydrophobic side of our Janus paper was applied to the wound bed (Figure 3b),

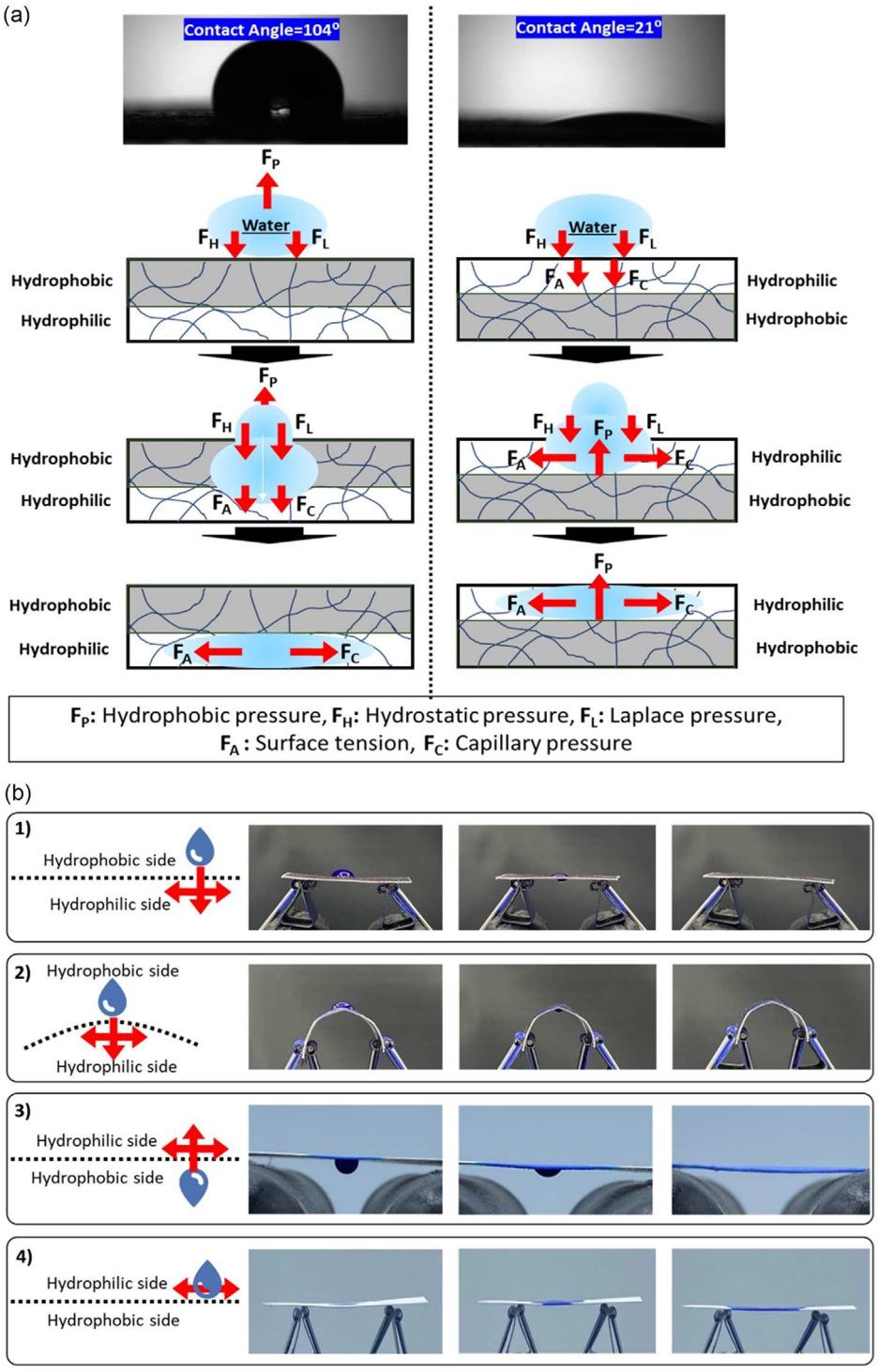

Figure 2. Characterization of water interaction with Janus Paper. a) Contact angle measurements: images showcasing a water droplet placed on (i) the hydrophobic side and (ii) the hydrophilic side of the Janus paper, demonstrating the surface wettability. b) Dynamic water transport study through the Janus paper, illustrated via sequential snapshots: 1) horizontal orientation with the hydrophobic side facing upward, observing water droplet behavior upon contact; 2) curved positioning with the water droplet applied to the upward-facing hydrophobic side, demonstrating water movement along the curvature; 3) inverted orientation (hydrophilic side facing upward) with water applied to the downward-facing hydrophobic side, examining water transfer to the hydrophilic surface; and 4) horizontal orientation with the hydrophilic side facing upward, observing water droplet behavior on direct contact.

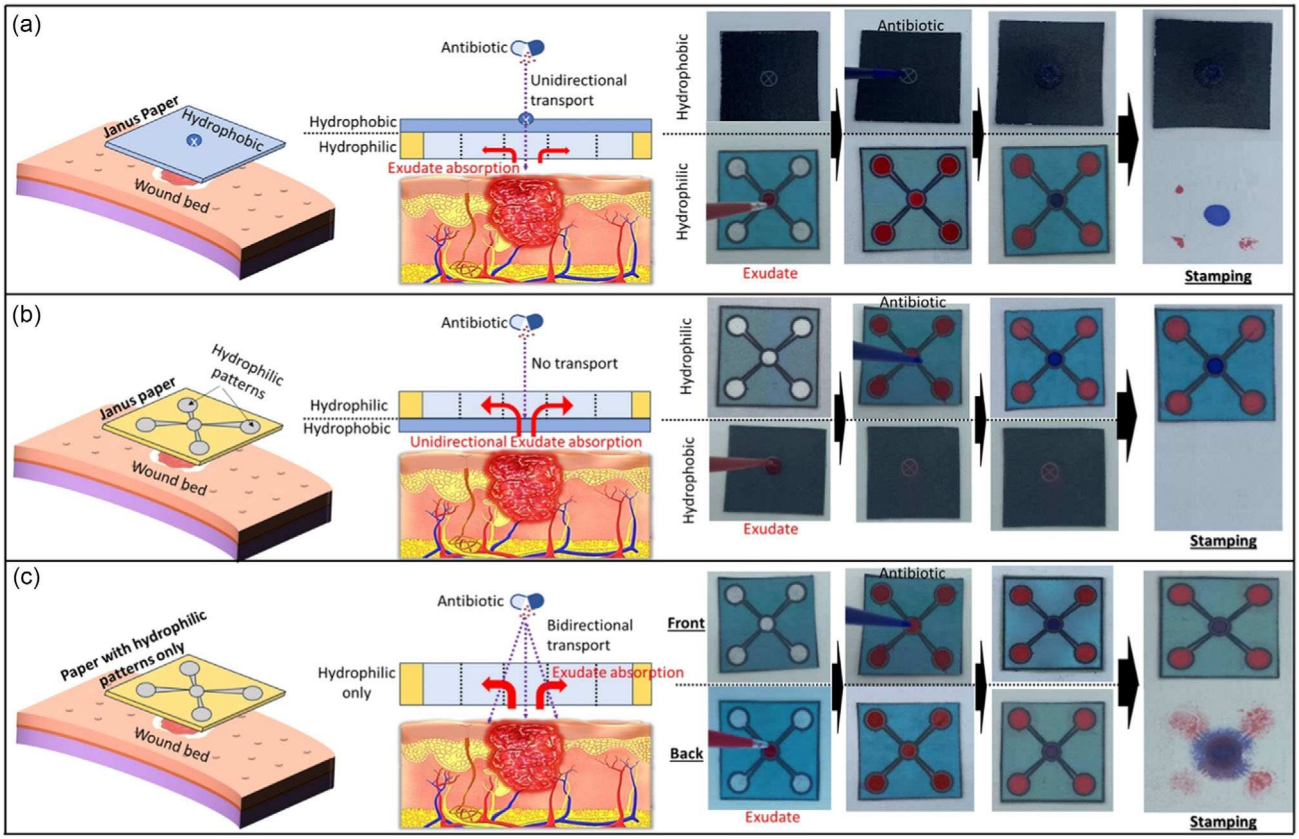

Figure 3. Comparative simulation of wound dressing configurations. This figure presents a series of schematic illustrations and corresponding photographs demonstrating simulations with different configurations of wound dressings. a) Janus paper oriented with the hydrophilic side facing the wound bed. This setup is intended to mimic the interaction of the dressing with wound exudates. b) Janus paper positioned with the hydrophobic side in contact with the wound bed. This arrangement allows for the assessment of liquid interaction dynamics from the opposite surface. c) A control setup using paper that only exhibits hydrophilic properties, serving as a baseline for comparison. In these simulations, red ink simulates wound exudate, while blue ink represents the antibiotic. Upon application of the blue ink, each wound dressing configuration is placed against a white paper background. This arrangement facilitates a clear visual assessment of antibiotic delivery efficiency and pattern to the simulated wound bed.

the blue ink was not delivered at all even though the red ink was unidirectionally absorbed and moved up to the hydrophilic regions through the hydrophobic part. As a control, a paper wound dressing only with hydrophilic patterns was prepared and simulated in the same way (Figure 3c). Each hydrophilic chamber was defined throughout the entire paper, possessing 22.6 µL of the volume in the middle and 35.3 µL of each pad. The paper sucked up the simulated exudate, but the antibiotic introduced through the middle chamber of the front side was not effectively delivered to the wound bed. The blue ink was not focused but spread over the wound bed, potentially decreasing the therapeutic effect, and generating a side effect by killing the beneficial skin microbiome.[6] Uncontrollable drug delivery may cause antibiotic resistance as well.

In our study, we sought to highlight the superior liquid retention properties of the Janus paper compared to standard wound care materials. To this end, we conducted a series of comparative experiments using commercially available gauze as a control. The results, vividly depicted in Figure S1, Supporting Information, offer a stark visual contrast between the performance of the two materials in handling liquid. In these experiments, colored ink, serving as a surrogate for wound exudate, was applied to both materials. When introduced to the commercial gauze, the ink rapidly dispersed and left conspicuous stains on the underlying surface, indicative of poor liquid containment. Conversely, the Janus paper exhibited a markedly different behavior. It not only absorbed the liquid but also effectively confined it within its structure, preventing any spread to the background substrate. This critical distinction highlights the Janus paper's bidirectional transport capabilities, which play a pivotal role in maintaining a drier and more conducive microenvironment for wound healing. The ability of the Janus paper to control liquid spread is particularly significant in the context of wound care. By preventing maceration and enhancing comfort, which are often challenges with traditional gauze dressings, the Janus paper offers a more advanced solution for wound management. It addresses the crucial need for effective exudate control, which is a key determinant of patient comfort and the success of wound healing outcomes. Our findings point to the Janus paper as a potential game-changer in wound care, offering significant advancements over conventional materials in managing wound exudates.

2.3. Evaluation of the Drug Delivery Efficiency

The efficiency of the drug delivery was evaluated by an agar diffusion test against the Gram-negative *Escherichia coli* presumably prevalent in infected wounds. The effective drug delivery will produce a zone where bacterial growth is inhibited. 2 μg L^{-1} each of the antibiotics ciprofloxacin, ceftazidime, and gentamicin were first applied against *E. coli* cultured overnight on agar (Figure S2, Supporting Information). *E. coli* exhibited high resistance to ceftazidime and gentamicin while ciprofloxacin inhibited bacterial growth. To determine the lowest ciprofloxacin concentration that can prevent the growth of *E. coli*, the inhibition zone was measured with decreasing antibiotic concentrations. Because the inhibition zone diameter with 0.5 μg L^{-1} ciprofloxacin did not show much difference from 0.4 μg L^{-1}, we selected 0.4 μg L^{-1} as a minimum inhibitory concentration to be applied to a simulated *E. coli* wound infection, which is very similar to the value from the Clinical and Laboratory Standards Institute (CLSI) guidelines (https://clsi.org/). To assess the delivery efficiency of the drug through different dressings, we first filled the hydrophilic patterns of each dressing with the red ink (assuming that the wound exudate wicked the dressing) and then placed the dressings on the agar plate cultured with *E. coli*. When the hydrophilic side of our Janus paper was laid face down on the agar, the antibiotic was introduced through the upward hydrophobic side. A very effective drug delivery was made, generating an obvious inhibition zone (**Figure 4**a). However, the antibiotic applied through the hydrophilic side of the Janus paper was not delivered to the bacterial culture without generating any inhibition zone (Figure 4b). Even when the antibiotic was dropped on the paper dressing only with hydrophilic patterns, no noticeable inhibition zone was developed (Figure 4c), indicating that the hydrophilic dressing blocks effective antibiotic delivery. This agrees with the results shown in Figure 3c.

The objective of this study was to unveil the promising capabilities of our Janus material through an exploratory investigation. Our primary focus centered on comprehensively understanding the fundamental properties and underlying mechanisms of the Janus membrane, utilizing both in vitro and ex vivo testing approaches. In the preceding section of our report, we detailed extensive in vitro testing which illuminated the dual functionality inherent in our design. This testing specifically highlighted the material's proficiency in sweat absorption and its capacity for targeted drug delivery. Following this, we conducted ex vivo experiments using porcine skin models. These tests were designed to closely mimic the conditions of an

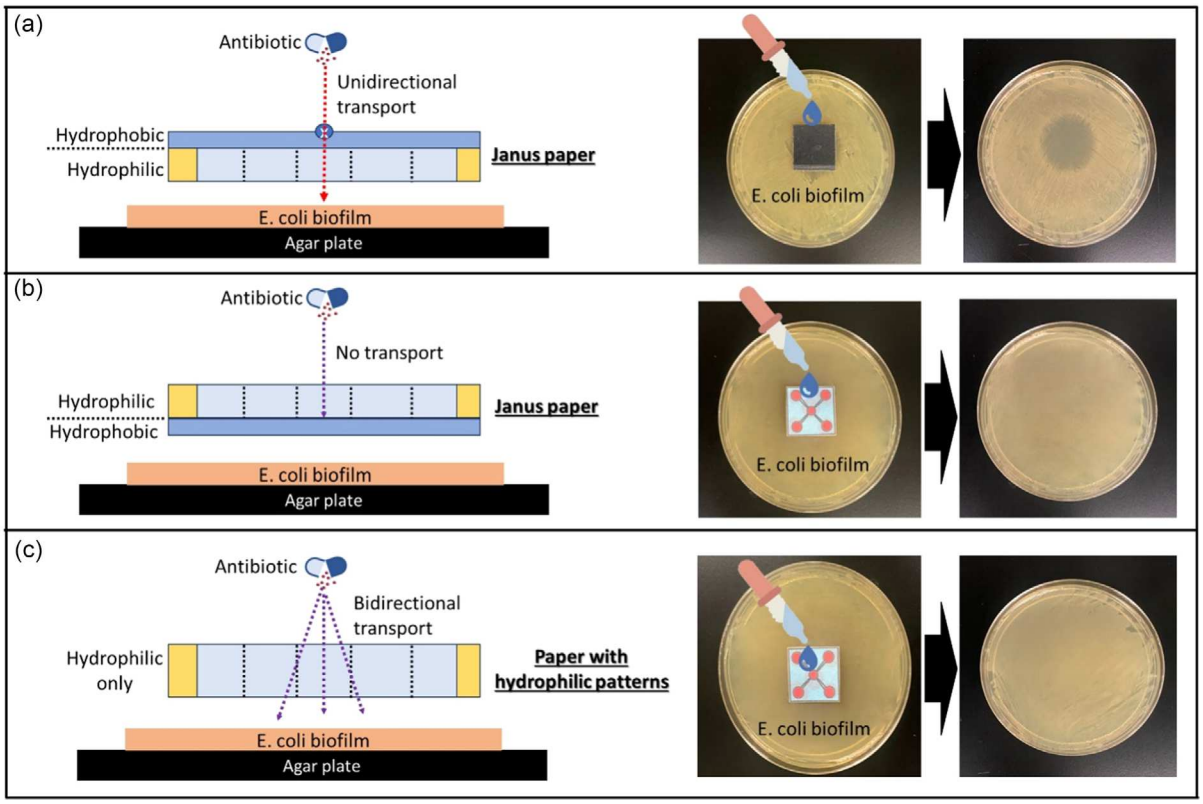

Figure 4. Evaluation of drug delivery efficiency in various wound dressing configurations. This figure includes schematic illustrations of the experimental setup used to assess the efficacy of drug delivery through different wound dressing designs. Accompanying optical images display the resultant zones of inhibition for each dressing type when tested against *E. coli* on agar plates infused with 0.4 μg L^{-1} ciprofloxacin: a) Janus paper oriented with the hydrophilic side in contact with the agar surface. This configuration aims to evaluate the efficiency of drug delivery from the hydrophilic aspect of the dressing. b) Janus paper positioned with the hydrophobic side facing the agar. This setup is designed to assess the drug delivery capabilities when the hydrophobic surface is in direct contact with the microbial culture. c) Control setup involving paper that only has hydrophilic properties. This comparison aims to benchmark the drug delivery efficiency of the Janus paper against a standard hydrophilic surface.

E. coli-infected wound, providing a more realistic assessment of the membrane's therapeutic potential in a simulated biological environment. Although in vivo animal models are the most suitable to preclinically assess the function of the wound dressing, the ex vivo simulation with porcine skin is a strong method to demonstrate the function, feasibility, and practicability of the dressing. From microscopic fluorescent images, we observed that the bacterial growth was significantly reduced when the antibiotic was applied to the hydrophobic side of the Janus paper (**Figure 5**a—position ① and 4a). When the antibiotic was introduced through the hydrophilic side of the Janus paper, it did not penetrate the hydrophobic layer and reach the potential wound bed (Figure 5a—position ② and 4b). Even the antibiotic applied to the control paper with hydrophilic patterns only did not effectively inhibit the bacterial growth and reproduction (Figure 5a—position ③ and 4c).

One of the critical aspects that can allow the widespread use of wound dressings is their disposability. This is very critical especially when the dressings deal with pathogens because of the potential risks of infections. Moreover, the potential leakage of the used antibiotics can promote antibiotic resistance.[32] Given that conventional wound dressings are made from nondisposable polymers,[9,10] paper-based wound dressings can be an excellent platform featuring their inherent disposable and biocompatible nature. As shown in Figure 5b, our Janus paper required only 21 s to be completely disposed of by incineration. Furthermore, our paper-based dressings are significantly cost-effective for their single-use applications.

3. Conclusion

In summary, we introduced an innovative wound dressing for effective absorption of the wound exudate and antibiotic delivery directly and efficiently to the wound bed. The revolutionary dressing integrated a Janus-type hydrophobic and hydrophilic asymmetric interface into a single sheet of paper. The paper, containing branched hydrophilic chambers connected by microfluidic channels, was placed on the wound bed, facilitating the absorption of the wound exudate while the exact dose of the right antibiotic was introduced from the hydrophobic side of the paper dressing and effectively delivered to the wound bed through the unidirectional transport. Because of the efficient draining of the excessive wound exudate from the middle hydrophilic chamber to the side absorbent chambers, the directional manipulation of the antibiotic across the hydrophobic–hydrophilic interface could be accomplished. The ex vivo simulation on the porcine skin demonstrated a significant inhibition of *E. coli* growth and reproduction as the antibiotic was effectively conveyed through our Janus wound dressing. Potentially, the outer hydrophobic region will prevent the invasion of the pathogens from the environment while the half-wet middle chamber contacting the wound bed will

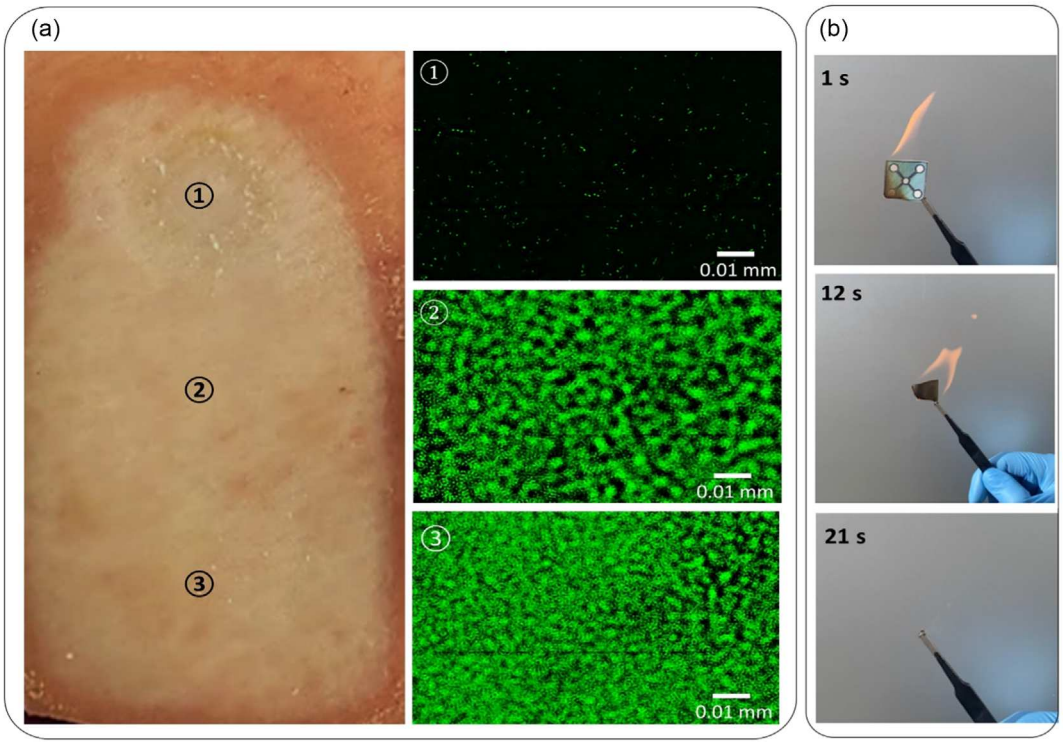

Figure 5. Ex vivo simulation and disposal methodology for Janus paper. a) This figure illustrates the ex vivo simulation using porcine skin to model wound treatment scenarios. *E. coli* bacteria were cultured overnight on the porcine skin to create a realistic infection environment. Subsequently, a concentration of 0.4 μg L^{-1} ciprofloxacin was administered using three different configurations of wound dressing materials: ① Janus paper applied with the hydrophilic side in direct contact with the skin, ② Janus paper oriented with the hydrophobic side facing the skin, and ③ control setup using paper featuring only hydrophilic patterns. b) This figure depicts the environmentally responsible disposal process of the Janus paper, highlighting its incineration.

maintain a moisture balance to promote cell regeneration and ultimately wound healing. Because the wound dressing was fully built up on a paper substrate, it was scalable, inexpensive, flexible, and wearable. Moreover, it could be easily disposed of by a simple incineration process.

4. Experimental Section

Preparation of the Janus Paper-Based Wound Dressings: The boundary wax patterns were defined on a 20 cm × 20 cm chromatography paper (Whatman 3 MM CHR) by using a solid-ink printer (Xerox Phaser, ColorQube 8570) and controlling the baking conditions. The wax patterns were designed using AutoCAD. The Janus membrane within the single sheet of paper was created by double-sided wax printing and subsequent heat treatment so that asymmetric hydrophobic and hydrophilic regions were formed across the paper thickness. The hydrophilic patterns with five chambers and four connecting channels were patterned on the front side of the paper, followed by the heat treatment at 150 °C for 40 s (Figure S3a, Supporting Information). Then, the wax was printed on the entire back side of the paper and heated in the same condition. Finally, an "x" mark was printed in the exact middle of the back side. The fabrication was scalable and mass-producible so that 16 wound dressings could be prepared on a single paper (Figure S3b, Supporting Information). The size of the hydrophilic chambers is shown in Figure S4, Supporting Information.

Bacterial Inoculum: *E. coli* was cultivated from −80 °C glycerol stock cultures by inoculating 20 mL of Luria Broth (LB) medium with gentle shaking in the air at 35 °C for 24 h. After incubation, the bacterial cells were harvested by centrifugation at 4000 rpm for 4 min, and the supernatant was discarded. The cells were then resuspended in a fresh LB medium to obtain the desired cell density, which was measured by monitoring the optical density at 600 nm.

Fluorescence Imaging: To monitor the bacterial growth and reproduction on porcine skin, the bacterial cells were conjugated with fluorescent dyes (carboxyfluorescein diacetate) and monitored under the fluorescence microscope (Ti-S 100 Nikon Microscope).

Measurement of Water Contact Angles: The water contact angles on the various dressings were determined with a Theta Lite contact angle meter (Theta Lite system, Biolin Scientific). A droplet of distilled water was deposited on each surface and the shape of the individual droplet was recorded and analyzed using ImageJ software.

Evaluation of Unidirectional Water Transfer Properties: All tests were performed by using safe and nontoxic food dyes. Red dye represents the wound exudate while blue dye represents the antibiotic.

Supporting Information

Supporting Information is available from the Wiley Online Library or from the author.

Acknowledgements

This work was supported by the National Science Foundation (ECCS #2246975 and CBET #2100757).

Conflict of Interest

The authors declare no conflict of interest.

Data Availability Statement

The data that support the findings of this study are available from the corresponding author upon reasonable request.

Keywords

directional antibiotic delivery, exudate absorption, hydrophobic–hydrophilic interface, Janus paper, paper-based wound dressings

Received: September 5, 2023
Revised: November 28, 2023
Published online: December 24, 2023

[1] L. Zhou, T. Min, X. Bian, Y. Dong, P. Zhang, Y. Wen, *ACS Appl. Bio Mater.* **2022**, *5*, 4055.
[2] S. Li, X. Wang, Z. Yan, T. Wang, Z. Chen, H. Song, Y. Zheng, *Adv. Sci.* **2023**, *10*, 2300576.
[3] L. Wang, L. Duan, G. Liu, J. Sun, M. Shahbazi, S. C. Kundu, R. L. Reis, B. Xiao, X. Yang, *Adv. Sci.* **2023**, *10*, 2207352.
[4] Z. Ming, L. Han, M. Bao, H. Zhu, S. Qiang, S. Xue, W. Liu, *Adv. Sci.* **2021**, *8*, 2102545.
[5] P. Mostafalu, A. Tamayol, R. Rahimi, M. Ochoa, A. Khalilpour, G. Kiaee, I. K. Yazdi, S. Bagherifard, M. R. Dokmeci, B. Ziaei, S. R. Sonkusale, A. Khademhosseini, *Small* **2028**, *14*, 1703509.
[6] L. Canchy, D. Kerob, A. Demessant, J. Amici, *J. Eur. Acad. Dermatol. Venereol.* **2023**, *37*, 7.
[7] S. Wang, W. Wu, J. C. C. Yeo, X. Y. D. Soo, W. Thitsartarn, S. Liu, B. H. Tan, A. Suwardi, Z. Li, Q. Zhu, X. J. Loh, *BMEMat* **2023**, *1*, e12021.
[8] D. Zhong, H. Zhang, Z. Ma, Q. Xin, Y. Lu, P. Shi, M. Qin, J. Li, C. Ding, *Front. Bioeng. Biotechnol.* **2022**, *10*, 1106267.
[9] Q. Zeng, X. Qi, G. Shi, M. Zhang, H. Haick, *ACS Nano* **2022**, *16*, 1708.
[10] R. Dong, B. Guo, *Nano Today* **2021**, *41*, 101290.
[11] L. Shi, X. Liu, W. Wang, L. Jiang, S. Wang, *Adv. Mater.* **2019**, *31*, 1804187.
[12] H. Pi, Y. Xi, J. Wu, M. Hu, B. Tian, Y. Yang, R. Wang, X. Zhang, *Chem. Eng. J.* **2023**, *455*, 140853.
[13] Y. Li, Y. Zhang, Y. Wang, K. Yu, E. Hu, F. Lu, S. Shang, R. Xie, G. Lan, *Chem. Eng. J.* **2022**, *429*, 131964.
[14] H. Zhang, C. Chen, H. Zhang, G. Chen, Y. Wang, Y. Zhao, *Appl. Mater. Today* **2021**, *23*, 101068.
[15] H. Wang, W. Duan, Z. Ren, X. Li, W. Ma, Y. Guan, F. Liu, L. Chen, P. Yan, X. Hou, *Adv. Healthcare Mater.* **2023**, *12*, 2202685.
[16] X. Zhang, R. Lv, L. Chen, R. Sun, Y. Zhang, R. Sheng, T. Du, Y. Li, Y. Qi, *ACS Appl. Mater. Interfaces* **2022**, *14*, 12984.
[17] J. Liu, M. Wu, J. Lu, Q. He, J. Zhang, *ACS Appl. Polym. Mater.* **2023**, *5*, 2596.
[18] E. Lee, H. Zhang, J. K. Jackson, C. J. Lim, M. Chiao, *RSC Adv.* **2016**, *6*, 79900.
[19] M. Song, Q. Zhao, X. Wang, C. Shi, X. Hu, J. Li, *Fibers Polym.* **2022**, *23*, 2511.
[20] H. Zhang, L. Sun, J. Guo, Y. Zhao, *Research* **2023**, *6*, 0129.
[21] L. Liu, H. Sun, J. Zhang, B. Xu, Y. Gao, D. Qi, Z. Mao, J. Wu, *Adv. Fiber Mater.* **2023**, *5*, 587.
[22] F. Bao, G. Pei, Z. Wu, H. Zhuang, Z. Zhang, Z. Huan, C. Wu, J. Chang, *Adv. Funct. Mater.* **2020**, *30*, 2005422.
[23] C. Llor, L. Bjerrum, *Ther. Adv. Drug Saf.* **2014**, *5*, 229.
[24] Z. Rafiee, S. Choi, *Analyst* **2023**, *148*, 2501.
[25] Y. Zhang, J. Yu, H. Zhang, Y. Li, L. Wang, *J. Appl. Polym. Sci.* **2022**, *139*, 52178.
[26] B. Jia, G. Li, E. Cao, J. Luo, X. Zhao, H. Huang, *Mater. Today Bio* **2023**, *19*, 100582, 2023.
[27] H. M. Nguyen, T. T. N. Le, A. T. Nguyen, H. N. T. Le, T. T. Pham, *RSC Adv.* **2023**, *13*, 5509.
[28] Y. Xu, Q. Fei, M. Page, G. Zhao, Y. Ling, S. B. Stoll, Z. Yan, *iScience* **2021**, *24*, 102736.

[29] M. Landers, A. Elhadad, M. Rezaie, S. Choi, *ACS Appl. Mater. Interfaces* **2022**, *14*, 45658.
[30] Y. Gao, S. Choi, *Adv. Mater. Technol.* **2023**, *3*, https://doi.org/10.1002/admt.202300396.
[31] J. Zhang, B. Liu, X. Liu, D. Wang, B. Dong, Y. Zhang, B. Xu, C. Chen, Z. Shen, *Macromol. Mater. Eng.* **2022**, *307*, 2200026.
[32] S. I. Polianciuc, A. E. Gurzău, B. Kiss, M. G. Ştefan, F. Loghin, *Med. Pharm. Rep.* **2020**, *93*, 231.